THE JOURNAL OF PHYSICAL CHEMISTRY Letters

Letter

pubs.acs.org/JPCL

Four Bases Score a Run: Ab Initio Calculations Quantify a Cooperative Effect of H-Bonding and π-Stacking on the Ionization Energy of Adenine in the AATT Tetramer

Ksenia B. Bravaya,[†] Evgeny Epifanovsky,[†,‡] and Anna I. Krylov*[,†]

[†]Department of Chemistry, University of Southern California, Los Angeles, California 90089-0482, United States

[‡]Department of Chemistry, University of California, Berkeley, California 94720, United States and Chemical Sciences Division, Lawrence Berkeley National Laboratory, Berkeley, California 94720, United States

Supporting Information

ABSTRACT: Benchmark calculations of the lowest ionized state of the $(A:T)_2$ (mixed adenine−thymine) cluster at the geometry taken from the DNA X-ray structure are presented. Vertical ionization energies (IEs) computed by the equation-of-motion coupled-cluster method with single and double substitutions are reported and analyzed. The shift in IE relative to the monomer (A) is −0.7 eV. The performance of the widely used B3LYP, ωB97X-D, and M06-2X functionals with respect to their ability to describe energetics and the character (localization versus delocalization) of the ionized states is also investigated. The shifts in IEs caused by H-bonding and stacking interactions are analyzed in terms of additive versus cooperative effects. It is found that the cooperative effect accounts for more than 20% of the shift in IE relative to the monomer. The cooperative effect and, consequently, the magnitude of the shift are well reproduced by the hybrid quantum mechanics/molecular mechanics scheme in which neutral thymine bases are represented by point charges.

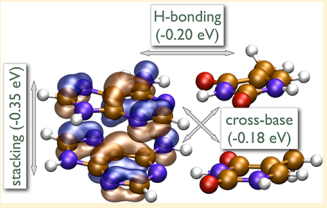

SECTION: Molecular Structure, Quantum Chemistry, and General Theory

Formation of ionized nucleic acid bases (NABs) is the primary step of DNA photo- and oxidative damage that can cause mutagenesis and initiate programmed cell death.[1,2] Once formed, the electron hole can propagate for a long distance along DNA's chain, initiating chemical processes far away from the original hole creation site.[3] Important for understanding a biologically relevant process, oxidative damage of DNA, charge transfer through DNA has also attracted attention in the context of nanotechnology applications. In particular, DNA has been considered as an important element in nanomaterial design, owing to its self-assembling ability. During the past decade, a number of artificial DNA-based 3D structures and nanomechanical devices were build.[4] Rothemund developed an algorithm for design of arbitrary DNA-based spatial structures.[5] The idea of using DNA π-stacked arrays as a one-dimensional conducting material was originally suggested by Eley and Spivey.[6] Although isolated DNA is found to be an insulator,[7] doped DNA in vacuum can be used as an electron-transferring material; ion transfer can be achieved by using solvated DNA.[7] All of these properties make DNA and its derivatives especially promising materials for nanoelectronics.[7,8]

Motivated by the above applications, a number of theoretical studies on ionized states of NABs,[9−19] their clusters,[20−28] and nucleotides and nucleosides[29−33] have been reported. In contrast to theoretical studies of NABs (monomers) and their dimers, for which highly accurate theoretical results are available, ab initio analysis of the ionized states of larger NAB aggregates has mainly employed density functional theory (DFT) methods.[34] These results should be taken with caution as standard DFT approaches tend to overestimate delocalization of the electron hole due to self-interaction error (SIE),[27,28] of which the H_2^+ dissociation curve is the most striking example.[35] SIE, which is present in most functionals, causes artificial stabilization of the delocalized charge[36−38] spoiling the description of Rydberg and charge-transfer excited states (see, for example, refs 39 and 40), vibronic interactions,[41,42] and charge distribution in the ground-state charge-transfer systems.[38] In the context of DNA, Mantz et al.[27] have shown that a correction for SIE is necessary for a qualitatively correct description of hole delocalization in stacked NAB dimers. On the basis of the comparison with the CASPT2 results, Voityuk et al.[43] concluded that hybrid functionals including B3LYP are appropriate for description of the character of the ionized state within a Kohn−Sham Koopmans-type scheme, that is, when the charge distribution of the hole is represented by the density of the highest occupied molecular orbital (HOMO) of the neutral. However, direct Kohn−Sham calculations of ionized species using the same functionals fail to predict the correct hole localization pattern.[43] Moreover, it is well-known that Koopmans ionization energies (IEs) are dramatically underestimated by many functionals. For example, the B3LYP HOMO energy of adenine is 6.4 eV, whereas the respective IE computed as the energy difference (ΔSCF) is about 8.4 eV. The M06-2X functional was reported to be successful in

Received: August 3, 2012
Accepted: September 5, 2012
Published: September 5, 2012

   dx.doi.org/10.1021/jz3011139 | J. Phys. Chem. Lett. 2012, 3, 2726−2732

Table 1. Vertical IEs (eV) of the Adenine Monomer and Dimer, the Mixed Adenine−Thymine (AT) Dimer, and the $(A:T)_2$ Tetramer[a]

	system						
method	A_g	AA_g	$AT(WC)_g$	$A1_{DNA}$	AA_{DNA}	$A1T1_{DNA}$	$AATT_{DNA}$
B3LYP/6-311+G(d,p)	8.37	7.82	7.88	8.29	7.62	7.91	7.25
B3LYP/6-311+G(df,pd)	8.38	7.83	7.89	8.29	7.63	7.91	7.27
ωB97X-D/6-311+G(d,p)	8.45	8.11	8.15	8.36	7.92	8.17	7.57
ωB97X-D/6-311+G(df,pd)	8.45	8.13	8.16	8.37	7.93	8.18	7.59
M06-2X/6-311+G(d,p)	8.62	8.26	8.33	8.36	8.05	8.35	7.71
M06-2X/6-311+G(df,pd)	8.64	8.29	8.35	8.37	8.07	8.37	7.74
EOM-IP-CCSD/6-31G	7.94	7.71	7.59	7.82	7.47	7.62	7.09
EOM-IP-CCSD/6-311+G(d,p)	8.35	8.02	8.01	8.21	7.81	8.01	

[a]IEs of the monomer and the dimers are computed at the geometries optimized for isolated species [A_g, AA_g, $AT(WC)_g$] as well as at the unrelaxed geometries taken from B-DNA ($A1_{DNA}$, AA_{DNA}, $A1T1_{DNA}$, $AATT_{DNA}$; see the computational details in the Supporting Information).

qualitative and quantitative description of ionized states of long stacks of DNA bases (adenine and guanine).[34] Long-range corrected functionals,[44−46] such as ωB97X[47] and BNL,[48] mitigate SIE and result in an improved description of ionized states.

The goal of this work is to provide high-level benchmark calculations of the IEs for model system of the stack of two AT (adenine−thymine) base pairs, AATT or $(A:T)_2$. The results are used to assess the accuracy and applicability of less computationally demanding approaches, such as DFT with the commonly used B3LYP functional as well as M06-2X and ωB97X-D.

Semiempirical model Hamiltonian methods are often used for theoretical description of the charge migration through the extended systems such as DNA chains[49−51] and molecular solids.[52,53] As input data, these methods require site energies, that is, the hole energy on a particular center, and coupling integrals. These quantities can be extracted from quantum chemical calculations. The overall accuracy of the charge migration rate depends critically on the accuracy of these parameters. Therefore, it is extremely important to have reliable reference data for model systems.[53] In addition, knowledge of the degree of the hole delocalization over neighboring bases is a prerequisite for appropriate choice of the quantum part in the QM/MM (quantum mechanics/molecular mechanics) calculations. For example, choosing too small a QM part will lead to artificial hole localization (and, of course, erroneous energetics) in the QM/MM calculations. In the context of ionized DNA, the important question is how many bases one needs to include in the QM part for a qualitatively correct description of an ionized state.

The equation-of-motion coupled cluster method for ionization potentials (EOM-IP-CCSD)[54−58] is the method of choice for the description of ionized states. In this approach, the problematic target open-shell wave functions are described by applying a Koopmans-like excitation operator $\hat{R}$ to the reference CCSD wave function representing a neutral closed-shell system

$$\Psi^{\mathrm{EOM-IP}}(N-1) = \hat{R}e^{\hat{T}}\Phi_0(N) \quad (1)$$

where $\Phi_0(N)$ is the reference determinant of the N-electron neutral system, $\hat{T}$ is the coupled cluster operator including single and double substitutions, and $\hat{R}$ consists of 1h and 2h1p (1 hole and 2 hole−1 particle) operators generating $(N-1)$-electron determinants from the N-electron reference. Amplitudes $\hat{T}$ are found by solving the CCSD equations for the ground-state wave function of the neutral, while amplitudes $\hat{R}$ are obtained by a subsequent diagonalization of the similarity transformed Hamiltonian, $\bar{H} = e^{-\hat{T}}He^{\hat{T}}$.

EOM-IP-CCSD does not suffer from spin contamination or symmetry breaking and simultaneously includes dynamical and nondynamical correlation. It describes multiple electronic states in one calculation and treats states with a different number of electrons on the same footing. In addition to IEs, EOM-IP-CCSD yields accurate energy splittings between the ionized states and smooth potential energy surfaces along charge-transfer coordinates.[57] This method has been successfully applied to describe the electronic structure of ionized benzene dimers,[58,59] water clusters[60−62] and nucleobases in the gas phase,[9] small clusters,[20−26] and species in bulk solvent.[63,64] In particular, EOM-IP-CCSD has been used to characterize hole delocalization in ionized noncovalent dimers.[20−22,24−26,58,59] We also employ a less expensive approximation to EOM-IP-CCSD, IP-CISD (configuration interaction with single and double substitutions for ionized states).[65]

Here, we present benchmark calculations of the lowest ionized states of the $(A:T)_2$ cluster at the geometry taken from the DNA X-ray structure.[66] We report the EOM-IP-CCSD vertical IE. We also compare the performance of widely used B3LYP as well as long-range and dispersion-corrected ωB97X-D[47,67] and meta-GGA M06-2X[68] functionals with respect to their ability to describe the energetics (i.e., IEs) and the character (localization versus delocalization) of the ionized states.

As adenine has a lower IE than thymine, the hole in the tetramer should be localized on A. An important question is how the interactions with the second A and with thymines affect the energy and the character of the ionized state. In our work on NAB dimers,[20−22,24−26] we interrogated the effect of π-stacking and H-bonding interactions on IEs and the hole shape. Owing to the complicated electronic structure of ionized states, one can expect significant nonadditive effects in larger clusters. Using the tetramer example, we analyze relative magnitudes of the IE shifts caused by H-bonding and stacking interactions in terms of additive versus cooperative effects. The latter is important for developing more realistic (in terms of computational cost) models for simulating charge-transfer processes in DNA. We also present the analysis of the shifts in terms of electrostatic interactions between the ionized and neutral fragments. Finally, we investigate whether the shift can be reproduced by a QM/MM calculation in which the two adenines are treated quantum-mechanically, whereas the thymine moieties are represented by point charges. In this

dx.doi.org/10.1021/jz3011139 | J. Phys. Chem. Lett. 2012, 3, 2726−2732

scheme, the wave function (QM part) is polarized by the electrostatic field of the MM (point charges) subsystem via Coulomb terms added to the one-electron QM Hamiltonian. These calculations enable a more quantitative and detailed analysis of the cooperative effect.

Table 1 presents the EOM-IP-CCSD IEs of the model systems at the geometry corresponding to the $(A:T)_2$ cluster carved from DNA, that is, $A1_{DNA}$, AA_{DNA}, $A1T1_{DNA}$, and $AATT_{DNA}$, as well as those for the optimized structures (A_g, AA_g, AT_g). A detailed description of the computational setup and model systems is given in the Supporting Information.

The MOs representing the lowest ionized states are shown in Figure 1. According to both EOM-IP-CCSD/6-31G and EOM-IP-CCSD/6-311+G(d,p), the lowest ionized state in all considered systems is of Koopmans character (i.e., the leading R_1 amplitudes are larger than 0.9), and therefore, the Hartree–Fock HOMO of the neutral represents the electron hole well.

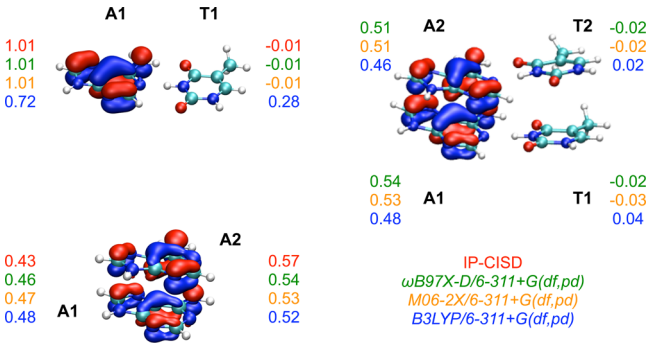

Figure 1. The Hartree–Fock HOMOs and the total positive charge (NBO) on each base in the dimers and tetramer according to the IP-CISD (red), ωB97X-D (green), M06-2X (orange), and B3LYP (blue) calculations. The 6-31+G(d,p) and 6-31G bases were used for the IP-CISD calculations of AA and A1T1, respectively.

As expected, the HOMO of the $A1T1_{DNA}$ dimer is composed of adenine's HOMO, that is, the hole is localized on A. Despite the low symmetry of our AA_{DNA} dimers, the hole is delocalized between the two bases and resides on the orbital that can be described as an out-of-phase linear combination of the HOMOs of the two A monomers. The shape of the HOMO of the $(A:T)_2$ tetramer is very similar to that of the AA dimers; the addition of the TT stacked pair does not affect the character of the ionized state. We also tested whether adding just one T may localize the hole on one of the adenines and found that the hole remains delocalized (the respective MOs are given in the Supporting Information).

The effects of H-bonding and stacking interactions on the IEs of the cluster are quantified in Figure 2. Both interactions have a pronounced effect on the IE of A; stacking interactions result in the decrease of IEs by stabilizing the hole via delocalization, whereas the electrostatic interactions are responsible for the IE decrease in the H-bonded dimer. This observation is in agreement with the results of the recent studies of the electronic structure of ionized states in the NAB dimers.[21,22,24−26] In the largest cluster, the tetramer, the bases experience both types of interactions, similar to the native DNA environment. Moreover, there are also interactions between A and T that are not H-bonded, that is, cross interactions between the bases. An important question for future studies of more complex and realistic systems is whether the delocalization of the hole remains the same as that in the stacked dimer

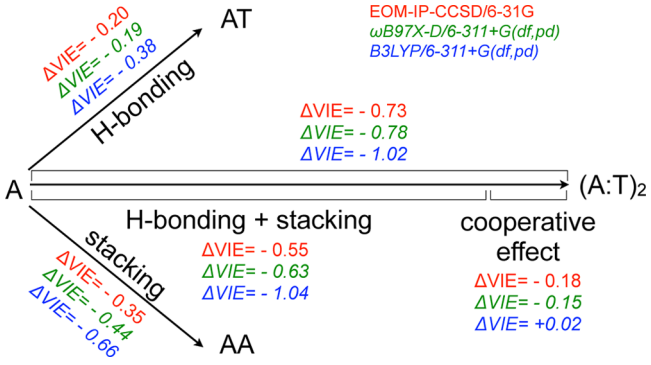

Figure 2. The effects of hydrogen bonding and stacking interactions on the IE of adenine and the additivity analysis using IP-CISD (red), ωB97X-D (green), and B3LYP (blue). Cooperative effects account for more than 20% of the IE shift at the EOM-IP-CCSD level. A, AT, AA, and $(A:T)_2$ correspond to A_{DNA}, $A1T1_{DNA}$, AA_{DNA}, and $AATT_{DNA}$ clusters, respectively.

and whether the changes in IEs due to H-bonding and π-stacking interactions are additive or there is a cooperative effect. Although the hole is delocalized over two adenines in the $(A:T)_2$ complex, one can expect similar shifts in IEs due to electrostatic interactions with T as only half of the charge resides on each adenine interacting with thymine. To test the additivity of these effects, we analyzed the shifts in IEs. Stacking interactions result in a shift of −0.35 eV. H-bonding causes a decrease in the IE of 0.20 eV. Therefore, assuming additivity of H-bonding and stacking interactions in the $AATT_{DNA}$ cluster, the estimated shift is −0.55 eV, to be compared with a computed shift of −0.73 eV (EOM-IP-CCSD). Therefore, 0.18 eV can be attributed to the cooperative H-bonding and π-stacking interactions. As illustrated by the analysis below, the cooperative effect is dominated by the electrostatic interactions between the non-H-bonded A1(A2) and T2(T1) bases (cross interactions); however, it also includes polarization contributions.

The origin of the cooperative effect is revealed by the analysis of charge–dipole interaction energies, similar to the one reported in ref 21 for AT and other NAB dimers. In this qualitative analysis, we replace the ionized moiety of the cluster (A1 or A2) by the NBO atomic point charges, whereas the neutral fragment is represented by its dipole moment, whose center is located at the molecular center of mass. We then compute the energy of charge–dipole interactions between the fragments as a sum over all atomic point charges

$$E = \sum_{i=1,N} \frac{q_i D}{|r_i|^2} \cos(\theta_i) \qquad (2)$$

where N is the number of atoms, q_i is the atomic point charge on the ith atom, D is the dipole moment of the neutral fragment, r is the vector connecting atom i with the center of mass of the neutral fragment, and θ is the angle between r and the dipole moment of the neutral fragment.

The results of this analysis are summarized in Figure 3. To assess whether the electrostatic cross interactions are responsible for the cooperative effects in the IEs shifts, we compared three quantities, (i) the charge–dipole interaction energy in the $A1T1_{DNA}$ ionized dimer and the difference between the IE of $A1T1_{DNA}$ and $A1_{DNA}$; (ii) the pairwise charge–dipole interaction energy in the $AATT_{DNA}$ cluster and the shift of $AATT_{DNA}$ relative to $A1_{DNA}$ with the subtracted

dx.doi.org/10.1021/jz3011139 | J. Phys. Chem. Lett. 2012, 3, 2726−2732

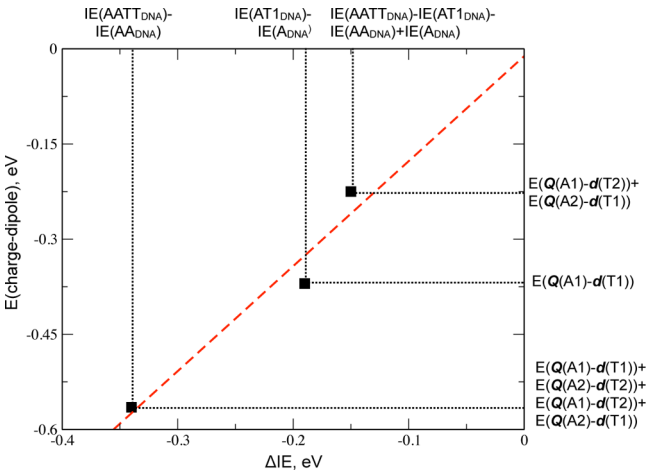

Figure 3. Comparison of the IE shifts with computed charge−dipole interaction energies in the three model systems: (i) the charge−dipole interaction energy in the A1T1$_{DNA}$ ionized dimer [$E(Q(A1) - d(T1)]$ and the shift in IE of A1T1$_{DNA}$ relative to A1$_{DNA}$ [IE(A1T1$_{DNA}$) − IE(A1$_{DNA}$)]; (ii) the AATT$_{DNA}$ cluster where only the effect of H-bonding is considered, for example, the pairwise charge−dipole interaction energy in the AATT$_{DNA}$ cluster, $E(Q(A1) - d(T1)) + E(Q(A2) - d(T2)) + E(Q(A1) - d(T2)) + E(Q(A2) - d(T1))$, is compared to the shift of AATT$_{DNA}$ relative to A1$_{DNA}$ with the subtracted contribution of the stacking interaction [IE(AATT$_{DNA}$) − IE(AA$_{DNA}$)]; and (iii) the AATT$_{DNA}$ cluster where only the cooperative effects are considered, for example, the energy of the electrostatic cross interactions between the bases $[E(Q(A1) - d(T2)) + E(Q(A2) - d(T1))]$ and the cooperative effect in the IE shifts [IE(AATT$_{DNA}$) − IE(AA$_{DNA}$) − IE(A1T1$_{DNA}$) + IE(A1$_{DNA}$)]. The red dashed line shows a linear fit of the data ($y = -0.011 + 1.66x$, $R^2 = 0.97$). ωB97X-D/6-311+G(df,pd) IEs are used.

contribution of the stacking interaction; and (iii) the energy of the electrostatic cross interactions between the bases and the cooperative effect in the IE shift. One can see that there is a reasonable correlation ($R^2 = 0.97$) between the electrostatic charge−dipole interaction energies and the observed shifts. Thus, we conclude that the electrostatic cross interaction between A1(A2) and T2(T1) is the dominant cause of the cooperative effect.

To gain a more quantitative insight into the cooperative effect, we performed a series of calculations with the QM/MM electronic embedding approach. In the lowest ionized state, the hole is localized on the two A units; therefore, we included one or both adenines in the QM part while representing thymines by point charges. This scheme accounts for QM/MM electrostatic interaction and polarization of the QM part by the MM subsystem (thymine point charges). The results of the EOM-IP-CCSD/6-31+G(d,p) QM/MM calculations are summarized in Table 2.

When we consider a single adenine in the QM part (such as in the A1:T1, A1:T2, A2:T1, or A2:T2 clusters), the shifts due to interaction with the H-bonded thymine and with the non-H-bonded thymine are similar (Table 2). For A2, the shifts are almost identical when either T1 (QM:A1/MM:T1) or T2 (QM:A1/MM:T2) is represented by point charges, that is, the shifts are −0.23 and −0.20 eV, respectively. Therefore, the combined electrostatic and QM polarization contributions to the IEs shifts (relative to the isolated A) due to the interactions of A with H-bonded T or non-H-bonded T are very similar in magnitude. This confirms that the cross interactions in the AATT$_{DNA}$ system are significant. For A1, the effect of adding

Table 2. QM/MM EOM-IP-CCSD/6-31+G(d,p)/Point Charges and Pure QM EOM-IP-CCSD/6-31G Vertical IEs (eV) of the Representative Adenine−Thymine Clusters with the Geometries Extracted from the AATT$_{DNA}$ system[a]

	EOM-IP-CCSD/6-31+G(d,p)			EOM-IP-CCSD/6-31G	
	IE, eV	ΔIE$_A$		IE, eV	ΔIE$_A$
A1$_{DNA}$	8.17	0.0	A1$_{DNA}$	7.82	0.0
QM:A1/MM:T1	7.91	−0.26	A1T1$_{DNA}$	7.62	−0.20
QM:A2/MM:T2	7.97	−0.20			
QM:A2/MM:T1	7.94	−0.23			
QM:A1/MM:T2	7.97	−0.20			
	IE, eV	ΔIE$_{AA}$		IE, eV	ΔIE$_{AA}$
AA$_{DNA}$	7.77	0.0	AA$_{DNA}$	7.47	
QM:A1A2/MM:T1	7.55	−0.22	AAT1$_{DNA}$	7.26	−0.21
QM:A1A2/MM:T2	7.57	−0.20			
QM:A1A2/MM:T1T2	7.30	−0.42	AATT$_{DNA}$	7.09	−0.38

[a]IEs are computed with one or two adenines included in the QM part and one or two thymines represented by point charges. Also shown are the shifts in IEs with respect to the A1$_{DNA}$ monomer, ΔIE$_A$, and AA$_{DNA}$ dimer, ΔIE$_{AA}$.

T1 (−0.26 eV shift) is slightly higher than that of adding T2 (−0.20 eV). This is probably due to a less favorable orientation of the T2 dipole moment relative to the hole density of the A1 ionized state.

In a larger model system with both adenines included into the quantum part, the shifts due to adding either T1 or T2 are essentially the same, −0.22 and −0.20 eV, respectively. We note that these AA−T interactions are additive and the resulting IE shift in the AATT$_{DNA}$ cluster with respect to AA$_{DNA}$ is −0.42 eV, which is exactly the sum of the IE shifts due to addition of each of the thymine moieties. Thus, the polarization of the QM electronic density by the MM part is not essential for this particular system, and the QM/MM interaction can be well-described by the electrostatic interaction of the AA hole density with the thymines' point charges. Nonsignificant polarization of the AA ionized state wave function by the electrostatic field of the thymines is consistent with similar shapes of the HOMOs of the AA:T1 and AA:T2 systems (Supporting Information, Figure S1).

Therefore, for a proper QM/MM description of the ionized DNA bases with the complementary strand in more realistic model systems of ionized DNA, it is necessary to account for electrostatics and hole delocalization over the stacked bases. Finally, we note that the IE shifts computed with the QM/MM scheme (EOM-IP-CCSD/6-31+G(d,p)) reproduce EOM-IP-CCSD/6-31G IEs with very good accuracy, −0.26 versus −0.20 eV and −0.42 versus −0.38 eV for A1T1$_{DNA}$ and AATT$_{DNA}$, respectively.

It is also informative to compare the performance of B3LYP, ωB97X-D, and M06-2X against the EOM-IP-CCSD and IP-CISD approaches. Figure 1 shows the NBO charge distribution over the ionized bases. ωB97X-D, M06-2X, and IP-CISD result in the hole being completely localized on A for the A1T1$_{DNA}$ dimer and nearly equally delocalized over the two A bases for the AA$_{DNA}$ dimer. Because the IP-CISD calculations for AATT$_{DNA}$ are expensive, the NBO analysis for this system was only performed using DFT. Because the charge distribution in AA$_{DNA}$ and A1T1$_{DNA}$ is very similar for ωB97X-D, M06-2X, and IP-CISD, we expect good agreement for the AATT$_{DNA}$ tetramer. On the basis of the ωB97X-D and M06-2X charge

dx.doi.org/10.1021/jz3011139 | J. Phys. Chem. Lett. 2012, 3, 2726−2732

distributions, we observe that the charge distribution in the tetramer is indeed very similar to that in AA_{DNA}. Importantly, due to SIE, B3LYP strongly overestimates delocalization of the ionized states, as follows, for example, from charge distribution for the $A1T1_{DNA}$ dimer, where B3LYP predicts 0.28*e* being located on T (relative to 0.01*e* predicted by IP-CISD). This delocalized ionized state manifests itself in the shifts of IEs, which are much higher for B3LYP than those for ωB97X-D and IP-CCSD for the AT systems, for example, 0.38 versus 0.19 eV for B3LYP and ωB97X-D, respectively. Moreover, the B3LYP shifts show no cooperative effect of H-bonding and π-stacking (Figure 2). Therefore, B3LYP is not an appropriate method for either a qualitative or quantitative description of ionized states of NAB clusters and related systems with competing H-bonding and stacking interactions. Interestingly, although ωB97X-D and M06-2X provide nearly identical charge distributions between the dimers and the tetramer (Figure 1), M06-2X overestimates the absolute values of the IEs by up to 0.36 and 0.17 eV, relative to the EOM-IP-CCSD and ωB97X-D values, respectively (6-311+G(d,p) basis, Table 1). Therefore, for the quantitative estimate of the tetramer's IE, we use the ωB97X-D value as described below.

The AA_{DNA} dimer is chosen as a model for the energy additivity scheme as it best represents the character of the ionized state of the $AATT_{DNA}$ system. The EOM-IP-CCSD/6-31G IE shift for the $AATT_{DNA}$ relative to AA_{DNA} is 0.38 eV. ωB97X-D/6-311+G(d,p) yields a similar shift of 0.35 eV and gives the IE value of 7.57 eV (for $AATT_{DNA}$). However, as one can see from Table 1, ωB97X-D/6-311+G(df,pd) tends to overestimate IEs for the monomers and dimers by ~0.2 eV. Two interpolation schemes can be used to obtain an estimate of the EOM-IP-CCSD/6-311+G(d,p) IE of the $AATT_{DNA}$ system. The first one is based on the basis set interpolation [EOM-IP-CCSD values are used, eq 3] and assumes that the basis set error is the same for the AA_{DNA} and $AATT_{DNA}$ systems. Indeed, the shifts in IE due to the basis set extension from 6-31G to 6-311+G(d,p) are nearly constant (0.4 eV) at the EOM-IP-CCSD level of theory for all considered clusters (Table 1). The second scheme is based on the method extrapolation [the same 6-311+G(d,p) basis set is used, eq 4]. Note that the IE shifts obtained with EOM-IP-CCSD/6-31G and ωB97X-D/6-311+G(d,p) are similar, and therefore, the two estimates are very close, 7.43 and 7.46 eV for interpolation schemes from eqs 3 and 4, respectively. The agreement between the two approaches validates the energy additivity schemes.

$$\mathrm{IE}^{\text{EOM-IP-CCSD/6-311+G(d,p)}}_{\mathrm{AATT_{DNA}}} \approx \mathrm{IE}^{\text{EOM-IP-CCSD/6-311+G(d,p)}}_{\mathrm{AA_{DNA}}} + \mathrm{IE}^{\text{EOM-IP-CCSD/6-31G}}_{\mathrm{AATT_{DNA}}} - \mathrm{IE}^{\text{EOM-IP-CCSD/6-31G}}_{\mathrm{AA_{DNA}}} \quad (3)$$

$$\mathrm{IE}^{\text{EOM-IP-CCSD/6-311+G(d,p)}}_{\mathrm{AATT_{DNA}}} \approx \mathrm{IE}^{\text{EOM-IP-CCSD/6-311+G(d,p)}}_{\mathrm{AA_{DNA}}} + \mathrm{IE}^{\omega\text{B97X-D/6-311+G(d,p)}}_{\mathrm{AATT_{DNA}}} - \mathrm{IE}^{\omega\text{B97X-D/6-311+G(d,p)}}_{\mathrm{AA_{DNA}}} \quad (4)$$

In summary, we report high-level quantum chemistry (EOM-IP-CCSD) benchmark calculations of IEs for the NAB tetramer $(A:T)_2$. The magnitude of the shift relative to adenine is −0.7 eV. Our best estimate of the absolute value of the vertical IE in the tetramer is 7.4 eV. Analysis of the relative magnitudes of the shift in IEs induced by H-bonding and stacking interactions reveals that there is a significant cooperative effect accounting for more than 20% of the total shift in adenine's IE. The cooperative effect is dominated by the electrostatic cross interactions (i.e., between adenine with a non-H-bonded thymine). Our calculations clearly show that at least two stacked NABs should be included into the quantum part for QM/MM simulations of DNA ionization due to the delocalized character of the ionized state. The results of the QM/MM calculations, in which two adenines are included in the QM and the thymines are described by point charges, agree well with the full EOM-IP-CCSD calculation. Therefore, one can expect that electronic embedding QM/MM schemes should reproduce cooperative effects with at least two stacked bases included in the quantum part.

Our calculations show that the ωB97X-D and M06-2X functionals provide a qualitatively correct description of the ionized state of the $(A:T)_2$ model system, ωB97X-D IEs being in slightly better agreement with the EOM-IP-CCSD values. The B3LYP functional provides a qualitatively incorrect picture of the ionized state due to SIE, leading to overestimation of the hole delocalization.

■ ASSOCIATED CONTENT

Ⓢ Supporting Information

Computational details and Cartesian coordinates of the model systems. This material is available free of charge via the Internet at http://pubs.acs.org.

■ AUTHOR INFORMATION

Notes

The authors declare no competing financial interest.

■ ACKNOWLEDGMENTS

This work is supported by the National Science Foundation through the CHE-0951634 grant. A.I.K. is a grateful recipient of the Bessel Research Award from the Humboldt Foundation, supporting her sabbatical stay at the University of Heidelberg. A.I.K. is deeply indebted to the Dornsife College of Letters, Arts, and Sciences and the WISE program (USC) for bridge funding support. The authors thank Mr. Jay Tanzman for providing a valuable insight into American sports and related idiomatic expressions.

■ REFERENCES

(1) Oka, S.; Ohno, M.; Tsuchimoto, D.; Sakumi, K.; Furuichi, M.; Nakabeppu, Y. Two Distinct Pathways of Cell Death Triggered by Oxidative Damage to Nuclear and Mitochondrial DNAs. *EMBO J.* **2008**, *27*, 421−432.

(2) Cadet, J.; Douiki, T.; Ravanat, J.-L. Oxidatively Generated Damage to the Guanine Moiety of DNA: Mechanistic Aspects and Formations in Cells. *Acc. Chem. Res.* **2008**, *41*, 1075−1083.

(3) Núñez, M.; Hall, D.; Barton, J. Long-Range Oxidative Damage to DNA: Effects of Distance and Sequence. *Chem. Biol.* **1999**, *6*, 85−97.

(4) Seeman, N. C. Nanomaterials Based on DNA. *Annu. Rev. Biochem.* **2010**, *79*, 65−87.

(5) Rothemund, P. W. K. Folding DNA to Create Nanoscale Shapes and Patters. *Nature* **2006**, *440*, 297−302.

(6) Eley, D. D.; Spivey, D. I. Semiconductivity of Organic Substances. Part 9. Nucleic Acid in the Dry State. *Trans. Faraday Soc.* **1962**, *58*, 411−415.

(7) Taniguchi, M.; Kawai, T. DNA Electronics. *Physica E* **2006**, *33*, 1−12.

(8) Genereux, J. C.; Barton, J. K. DNA Charges Ahead. *Nat. Chem.* **2009**, *1*, 106−107.

(9) Bravaya, K.; Kostko, O.; Dolgikh, S.; Landau, A.; Ahmed, M.; Krylov, A. Electronic Structure and Spectroscopy of Nucleic Acid Bases: Ionization Energies, Ionization-Induced Structural Changes, and Photoelectron Spectra. *J. Phys. Chem. A* **2010**, *114*, 12305−12317.
(10) Trofimov, A.; Schirmer, J.; Kobychev, V.; Potts, A.; Holland, D.; Karlsson, L. Photoelectron Spectra of the Nucleobases Cytosine, Thymine and Adenine. *J. Phys. B* **2006**, *39*, 305−329.
(11) Satzger, H.; Townsend, D.; Stolow, A. Reassignment of the Low Lying Cationic States in Gas Phase Adenine and 9-methyl Adenine. *Chem. Phys. Lett.* **2006**, *430*, 144−148.
(12) Zaytseva, I. L.; Trofimov, A. B.; Schirmer, J.; Plekan, O.; Feyer, V.; Richter, R.; Coreno, M.; Prince, K. C. Theoretical and Experimental Study of Valence-Shell Ionization Spectra of Guanine. *J. Phys. Chem. A* **2009**, *113*, 15142−15149.
(13) Dolgounitcheva, O.; Zakrzewski, V.; Ortiz, J. Ionization Energies and Dyson Orbitals of Thymine and Other Methylated Uracils. *J. Phys. Chem. A* **2002**, *106*, 8411−8416.
(14) Dolgounitcheva, O.; Zakrzewski, V.; Ortiz, J. Electron Propagator Calculations on Uracil and Adenine Ionization Energies. *Int. J. Quantum Chem.* **2000**, *80*, 831−835.
(15) Dolgounitcheva, O.; Zakrzewski, V. G.; Ortiz, J. V. Electron Propagator Theory of Guanine and its Cations: Tautomerism and Photoelectron Spectra. *J. Am. Chem. Soc.* **2000**, *122*, 12304−12309.
(16) Dolgounitcheva, O.; Zakrzewski, V. G.; Ortiz, J. V. Ionization Energies and Dyson Orbitals of Cytosine and 1-Methylcytosine. *J. Phys. Chem. A* **2003**, *107*, 822−828.
(17) Roca-Sanjuán, D.; Rubio, M.; Merchán, M.; Serrano-Andrés, L. Ab Initio Determination of the Ionization Potentials of DNA and RNA Nucleobases. *J. Chem. Phys.* **2006**, *125*, 084302.
(18) Dolgounitcheva, O.; Zakrzewski, V. G.; Ortiz, J. V. Vertical Ionization Energies of Adenine and 9-Methyl Adenine. *J. Phys. Chem. A* **2009**, *113*, 14630−14635.
(19) Zhang, L.; Pan, Y.; Qi, F. Theoretical Studies on Photoionization of Guanine Tautomers and Interconversion of Guanine Radicals. *J. Theor. Comput. Chem.* **2009**, *8*, 1103−1115.
(20) Golan, A.; Bravaya, K.; Kudirka, R.; Leone, S.; Krylov, A.; Ahmed, M. Ionization of Dimethyluracil Dimers Leads to Facile Proton Transfer in the Absence of H-Bonds. *Nat. Chem.* **2012**, *4*, 323−329.
(21) Bravaya, K.; Kostko, O.; Ahmed, M.; Krylov, A. The Effect of π-Stacking, H-Bonding, And Electrostatic Interactions on the Ionization Energies of Nucleic Acid Bases: Adenine−Adenine, Thymine−Thymine and Adenine−Thymine Dimers. *Phys. Chem. Chem. Phys.* **2010**, *12*, 2292−2307.
(22) Kostko, O.; Bravaya, K.; Krylov, A.; Ahmed, M. Ionization of Cytosine Monomer and Dimer Studied by VUV Photoionization and Electronic Structure Calculations. *Phys. Chem. Chem. Phys.* **2010**, *12*, 2860−2872.
(23) Khistyaev, K.; Bravaya, K.; Kamarchik, E.; Ahmed, O. K. M.; Krylov, A. The Effect of Microhydration on Ionization Energies of Thymine. *Faraday Discuss.* **2011**, *150*, 313−330.
(24) Zadorozhnaya, A.; Krylov, A. Zooming into π-Stacked Manifolds of Nucleobases: Ionized States of Dimethylated Uracil Dimers. *J. Phys. Chem. A* **2010**, *114*, 2001−2009.
(25) Golubeva, A.; Krylov, A. The Effect of π-stacking and H-bonding on Ionization Energies of a Nucleobase: Uracil Dimer Cation. *Phys. Chem. Chem. Phys.* **2009**, *11*, 1303−1311.
(26) Zadorozhnaya, A.; Krylov, A. Ionization-Induced Structural Changes in Uracil Dimers and Their Spectroscopic Signatures. *J. Chem. Theory Comput.* **2010**, *6*, 705−717.
(27) Mantz, Y.; Gervasio, F.; Laino, T.; Parrinello, M. Charge Localization in Stacked Radical Cation DNA Base Pairs And the Benzene Dimer Studied by Self-Interaction Corrected Density-Functional Theory. *J. Phys. Chem. A* **2007**, *111*, 105−112.
(28) Paukku, Y.; Hill, G. Theoretical Determination of One-Electron Redox Potentials for DNA Bases, Base Pairs, and Stacks. *J. Phys. Chem. A* **2011**, *115*, 4804−4810.
(29) Kim, N. S.; LeBreton, P. R. UV Photoelectron and Ab initio Quantum Mechanical Evaluation of Nucleotide Ionization Potentials in Water−Counterion Environments: π Polarization Effects on DNA Alkylation by Carcinogenic Methylating Agents. *J. Am. Chem. Soc.* **1996**, *118*, 3694−3707.
(30) Crespo-Hernández, C.; Close, D.; Gorb, L.; Leszczynski, J. Determination of Redox Potentials for the Watson−Crick Base Pairs, DNA Nucleosides, and Relevant Nucleoside Analogues. *J. Phys. Chem. B* **2007**, *111*, 5386−5395.
(31) Close, D. M.; Ohman, K. T. Ionization Energies of the Nucleotides. *J. Phys. Chem. A* **2008**, *112*, 11207−11212.
(32) Slavíček, P.; Winter, B.; Faubel, M.; Bradforth, S.; Jungwirth, P. Ionization Energies of Aqueous Nucleic Acids: Photoelectron Spectroscopy of Pyrimidine Nucleosides and Ab initio Calculations. *J. Am. Chem. Soc.* **2009**, *131*, 6460−6467.
(33) Pluhařová, E.; Jungwirth, P.; Bradforth, S. E.; Slavíček, P. Ionization of Purine Tautomers in Nucleobases, Nucleosides, and Nucleotides: From the Gas Phase to the Aqueous Environment. *J. Phys. Chem. B* **2011**, *115*, 1294.
(34) Kumar, A.; Sevilla, M. Density Functional Theory Studies of the Extent of Hole Delocalization in One-Electron Oxidized Adenine and Guanine Base Stacks. *J. Phys. Chem. B* **2011**, *115*, 4990−5000.
(35) Bally, T.; Sastry, G. Incorrect Dissociation Behavior of Radical Ions in Density Functional Calculations. *J. Phys. Chem. A* **1997**, *101*, 7923−7925.
(36) Polo, V.; Kraka, E.; Cremer, D. Electron Correlation and the Self-Interaction Error of Density Functional Theory. *Mol. Phys.* **2002**, *100*, 1771−1790.
(37) Zhang, Y.; Yang, W. A Challenge for Density Functionals: Self-Interaction Error Increases for Systems with a Noninteger Number of Electrons. *J. Chem. Phys.* **1998**, *109*, 2604−2608.
(38) Lundber, M.; Siegbahn, P. Quantifying the Effects of the Self-Interaction Error in DFT: When do the Delocalized States Appear? *J. Chem. Phys.* **2005**, *122*, 224103.
(39) Dreuw, A.; Head-Gordon, M. Single-Reference Ab Initio Methods for the Calculation of Excited States of Large Molecules. *Chem. Rev.* **2005**, *105*, 4009−4037.
(40) Dreuw, A.; Head-Gordon, M. Comment on: 'Failure of Time-Dependent Density Functional Methods for Excitations in Spatially Separated Systems' by Wolfgang Hieringer and Andreas Gorling. *Chem. Phys. Lett.* **2006**, *426*, 231−233.
(41) Slipchenko, L.; Krylov, A. Efficient Strategies for Accurate Calculations of Electronic Excitation and Ionization Energies: Theory and Application to the Dehydro-meta-xylylene Anion. *J. Phys. Chem. A* **2006**, *110*, 291−298.
(42) Vanovschi, V.; Krylov, A.; Wenthold, P. Structure, Vibrational Frequencies, Ionization Energies, and Photoelectron Spectrum of the Para-benzyne Radical Anion. *Theor. Chim. Acta* **2008**, *120*, 45−58.
(43) Félix, M.; Voityuk, A. DFT Performance for the Hole Transfer Parameters in DNA π-stacks. *Int. J. Quantum Chem.* **2011**, *111*, 191201.
(44) Iikura, H.; Tsuneda, T.; Yanai, T.; Hirao, K. A Long-Range Correction Scheme for Generalized-Gradient-Approximation Exchange Functionals. *J. Chem. Phys.* **2001**, *115*, 3540.
(45) Rohrdanz, M.; Martins, K.; Herbert, J. A Long-Range-Corrected Density Functional That Performs Well for Both Ground-State Properties and Time-Dependent Density Functional Theory Excitation Energies, Including Charge-Transfer Excited States. *J. Chem. Phys.* **2009**, *130*, 054112.
(46) Baer, R.; Livshits, E.; Salzner, U. Tuned Range-Separated Hybrids in Density Functional Theory. *Annu. Rev. Phys. Chem.* **2010**, *61*, 85−109.
(47) Chai, J.; Head-Gordon, M. Systematic Optimization of Long-Range Corrected Hybrid Density Functionals. *J. Chem. Phys.* **2008**, *128*, 084106.
(48) Baer, R.; Neuhauser, D. Density Functional Theory With Correct Long-Range Asymptotic Behavior. *Phys. Rev. Lett.* **2005**, *94*, 043002.
(49) Conwell, E.; Rakhmanova, S. Polarons in DNA. *Proc. Nat. Acad. Sci. U.S.A.* **2000**, *97*, 4556.

(50) Gutiérrez, R.; Mandal, S.; Cuniberti, G. Dissipative Effects in the Electronic Transport through DNA Molecular Wires. *Phys. Rev. B* **2005**, *71*, 235116.
(51) Roche, S. Sequence Dependent DNA-Mediated Conduction. *Phys. Rev. Lett.* **2003**, *91*, 108101.
(52) Valeev, E.; Coropceanu, V.; da Silva Filho, D.; Salman, S.; Brédas, J.-L. Effect of Electronic Polarization on Chrage-Transport Parameters in Molecular Organic Semiconductors. *J. Am. Chem. Soc.* **2006**, *128*, 9882−9886.
(53) Zhang, J.; Valeev, E. Hybrid One-Electron/Many-Electron Methods for Ionized States of Molecular Clusters. *Phys. Chem. Chem. Phys.* **2012**, *14*, 7863−7871.
(54) Pal, S.; Rittby, M.; Bartlett, R.; Sinha, D.; Mukherjee, D. Multireference Coupled-Cluster Methods Using an Incomplete Model Space — Application to Ionization-Potentials and Excitation-Energies of Formaldehyde. *Chem. Phys. Lett.* **1987**, *137*, 273−278.
(55) Stanton, J.; Gauss, J. Analytic Energy Derivatives for Ionized States Described by the Equation-of-Motion Coupled Cluster Method. *J. Chem. Phys.* **1994**, *101*, 8938−8944.
(56) Kamiya, M.; Hirata, S. Higher-Order Equation-of-Motion Coupled-Cluster Methods for Ionization Processes. *J. Chem. Phys.* **2006**, *125*, 074111−074125.
(57) Pieniazek, P.; Arnstein, S.; Bradforth, S.; Krylov, A.; Sherrill, C. Benchmark Full Configuration Interaction and EOM-IP-CCSD Results for Prototypical Charge Transfer Systems: Noncovalent Ionized Dimers. *J. Chem. Phys.* **2007**, *127*, 164110.
(58) Pieniazek, P.; Bradforth, S.; Krylov, A. Charge Localization and Jahn−Teller Distortions in the Benzene Dimer Cation. *J. Chem. Phys.* **2008**, *129*, 074104.
(59) Pieniazek, P.; Krylov, A.; Bradforth, S. Electronic Structure of the Benzene Dimer Cation. *J. Chem. Phys.* **2007**, *127*, 044317.
(60) Pieniazek, P.; VandeVondele, J.; Jungwirth, P.; Krylov, A.; Bradforth, S. Electronic Structure of the Water Dimer Cation. *J. Phys. Chem. A* **2008**, *112*, 6159−6170.
(61) Pieniazek, P.; Sundstrom, E.; Bradforth, S.; Krylov, A. The Degree of Initial Hole Localization/Delocalization in Ionized Water Clusters. *J. Phys. Chem. A* **2009**, *113*, 4423−4429.
(62) Kamarchik, E.; Kostko, O.; Bowman, J.; Ahmed, M.; Krylov, A. Spectroscopic Signatures of Proton Transfer Dynamics in the Water Dimer Cation. *J. Chem. Phys.* **2010**, *132*, 194311.
(63) Ghosh, D.; Isayev, O.; Slipchenko, L.; Krylov, A. The Effect of Solvation on Vertical Ionization Energy of Thymine: From Microhydration to Bulk. *J. Phys. Chem. A* **2011**, *115*, 6028−6038.
(64) Ghosh, D.; Roy, A.; Seidel, R.; Winter, B.; Bradforth, S.; Krylov, A. A First-Principle Protocol for Calculating Ionization Energies and Redox Potentials of Solvated Molecules and Ions: Theory and Application to Aqueous Phenol and Phenolate. *J. Phys. Chem. B* **2012**, *116*, 72697280.
(65) Golubeva, A.; Pieniazek, P.; Krylov, A. A New Electronic Structure Method for Doublet States: Configuration Interaction in the Space of Ionized 1h and 2h1p Determinants. *J. Chem. Phys.* **2009**, *130*, 124113.
(66) Narayana, N.; Weiss, M. Crystallographic Analysis of a Sex-Specific Enhancer Element: Sequence-Dependent DNA Structure, Hydration, and Dynamics. *J. Mol. Biol.* **2009**, *385*, 469−490.
(67) Chai, J.; Head-Gordon, M. Long-Range Corrected Hybrid Density Functionals with Damped Atom−Atom Dispersion Interactions. *Phys. Chem. Chem. Phys.* **2008**, *10*, 6615−6620.
(68) Truhlar, D. The M06 Suite of Density Functionals for Main Group Thermochemistry, Thermochemical Kinetics, Noncovalent Interactions, Excited States, and Transition Elements: Two New Functionals and Systematic Testing of Four M06-Class Functionals and 12 Other Functionals. *Theor. Chim. Acta* **2008**, *120*, 215241.